Application of Numerical Ship Navigation in a Coastal Area

Chen Chen
Faculty of Maritime Science, Kobe University,
Higashinada-ku, Kobe, Japan.
cc198895@hotmail.com

Shigeaki SHIOTANI
Organization of Advanced Science and Technology,
Higashinada-ku, Kobe, Japan.
shiotani@maritime.kobe-u.ac.jp

Kenji Sasa
Faculty of Maritime Science, Kobe University,
Higashinada-ku, Kobe, Japan.
sasa@maritime.kobe-u.ac.jp

Abstract:

Waves, ocean currents, and sea surface winds are important factors for safe and economic ship navigation, especially in coastal areas where ship density is relatively higher and the topography is more complicated. In this research, Osaka Bay, Japan, was selected as a location to conduct a representative, low-pressure numerical ship navigation. WRF, SWAN, and POM models were used to produce numerical simulations of wind, waves, and currents, respectively. The high-resolution weather and ocean information was then used to conduct a numerical ship navigation. To verify the accuracy, the results simulating the weather and ocean were compared with actual observation data. The findings showed that the estimation of a ship's position using the proposed numerical navigation simulation method was effective in helping a ship navigate safely and economically.

Keywords: Waves; Wind; Current; Coastal area; Numerical ship navigation

I. INTRODUCTION

With the increasing influence of global warming, typhoons are becoming larger and stronger, leading to more high-wave areas in the ocean. Therefore, vessel navigation will involve greater risks in high-frequency typhoon areas, such as the East China Sea and the Japanese coastal area. Besides weather routing for oceangoing ships, navigators in coastal areas need exact weather and ocean forecasts because of more complex topography and higher ship density.

As a busy shipping area, Osaka Bay, Japan, was chosen as a location to study numerical ship navigation based on weather and ocean simulation. To determine the effects weather and the ocean have on a sailing ship, the ocean currents, waves, and wind were studied when a representative typhoon was passing the Osaka Bay area.

Several modernized weather and ocean models, such as WRF (Weather Research & Forecasting Model) (Mase, H., Katsui, S., Yasuda, T., Tomand, T.H., and Ogawa, K., 2006; Carvalho, D., Rocha, A., Gomez-Gesteira, M., and Santos, C., 2012), SWAN (Simulating Waves Nearshore) (Booji, N. et al., 1999; The SWAN Team, 2009), and POM (Princeton Ocean Model) (Blumberg, A.F., and Mellor, G.L., 1987; Mellor, G.L., 1998), were utilized to obtain the high-resolution data, which was then applied to another model, MMG (Mathematical Model Group) (Yoshimura, Y., 1986), to make the numerical ship navigation to estimate a ship's position under weather and ocean influences.

II. MODEL DESCRIPTION

A. Weather Research & Forecasting Model

978-0-933957-40-4 ©2013 MTS

In this paper, a wind simulation was carried out by WRF-ARW 3.3.1, a mesoscale meteorological model developed principally by the National Center for Atmospheric Research (NCAR), the National Oceanic and Atmospheric Administration, the National Centers for Environmental Prediction (NCEP), the Forecast Systems Laboratory (FSL), the Air Force Weather Agency (AFWA), the Naval Research Laboratory, the University of Oklahoma, and the Federal Aviation Administration (FAA).

Set with a fully compressible, Eulerian, non-hydrostatic equation set with a run-time hydrostatic option, the model can predict three-dimensional wind momentum components, surface pressure, dew point, precipitation, surface-sensible and latent heat fluxes, relative humidity, and air temperature on a sigma-pressure, vertical coordinate grid. The time integration scheme in the model uses the third-order Runge-Kutta scheme, and the spatial discretization employs 2nd to 6th order schemes.

As boundary information, GFS-FNL data were used. The GFS (Global Forecast System) is run operationally four times a day in near-real time at NCEP. GFS-FNL (Final) Operational Global Analysis data are available on 1.0x1.0-degree grids every six hours.

B. Princeton Ocean Model

The Princeton Ocean Model was used to simulate the current affected by this typhoon. This three-dimensional, primitive-equation ocean model includes thermodynamics and the Mellor-Yamada level 2.5 turbulence closure and uses a sigma coordinate in the vertical to resolve the variation of bottom topography. The basic equations to calculate the tidal current are the continuity equation and the Navier-Stokes equation:

$$\begin{cases} \frac{\partial DU}{\partial_x} + \frac{\partial DV}{\partial_y} + \frac{\partial_\omega}{\partial_t} + \frac{\partial_\gamma}{\partial_T} = 0 \\ \frac{\partial UD}{\partial_t} + \frac{\partial U^2 D}{\partial_x} + \frac{\partial UVD}{\partial_y} + \frac{\partial U\omega}{\partial_\sigma} - fVD + gD\frac{\partial_\gamma}{\partial_x} \\ + \frac{gD^2}{\rho_0}\int_\sigma^0 \left[\frac{\partial_\rho'}{\partial_x} - \frac{\sigma'}{D}\frac{\partial D}{\partial_x}\frac{\partial_\rho'}{\partial_\sigma'}\right] d\sigma' = \frac{\partial}{\partial_\sigma}\left[\frac{K_M}{D}\frac{\partial U}{\partial_\sigma}\right] + F_x \\ \frac{\partial UD}{\partial_t} + \frac{\partial UVD}{\partial_x} + \frac{\partial V^2 D}{\partial_y} + \frac{\partial V\omega}{\partial_\sigma} + fUD + gD\frac{\partial_\gamma}{\partial_y} \\ + \frac{gD^2}{\rho_0}\int_\sigma^0 \left[\frac{\partial_\rho'}{\partial_y} - \frac{\sigma'}{D}\frac{\partial D}{\partial_y}\frac{\partial_\rho'}{\partial_\sigma'}\right] d\sigma' = \frac{\partial}{\partial_\sigma}\left[\frac{K_M}{D}\frac{\partial V}{\partial_\sigma}\right] + F_y \end{cases} \quad (1)$$

where U and V are the components of the horizontal velocity of a tidal current, ω is the velocity component of the normal direction to the σ plain, f is the Coriolis coefficient, g is the acceleration of gravity, F_x and F_y are the horizontal viscosity diffusion coefficients, and K_M is the frictional coefficient of the sea bottom.

C. Simulating WAves Nearshore

As a numerical model for simulating waves, SWAN was used. Implemented with the wave spectrum method, SWAN is a third-generation wave model that can compute random, short-crested, wind-generated waves in coastal regions as well as inland waters. The SWAN model is used to solve the spectral action balance equation without prior restrictions on the spectrum for the effects of spatial propagation, refraction, reflection, shoaling, generation, dissipation, and nonlinear wave-wave interactions. After being satisfactorily verified with field measurements, it is considered to be an ideal candidate as a reliable simulation model of typhoon waves in coastal waters once a typhoon's cyclonic wind fields have been determined.

Consequently, the SWAN model is suitable for estimating waves in bay areas with shallow water and ambient currents. Information about the sea surface is contained in the wave variance spectrum of energy density $E(\sigma, \theta)$. Wave energy is distributed over frequencies (θ) and propagation directions (σ). σ is observed in a frame of reference moving with the current velocity, and θ is the direction normal to the wave crest of each spectral component. The expressions for these propagation speeds are taken from linear wave theory (e.g., Whitham, 1974; Dingemans, 1997), while diffraction is not considered in the model. The action balance equation of the SWAN model in Cartesian coordinates is as follows:

$$\frac{\partial}{\partial x}c_x N + \frac{\partial}{\partial y}c_y N + \frac{\partial}{\partial \sigma}c_\sigma N + \frac{\partial}{\partial \theta}c_\theta N = \frac{S}{\sigma} \quad (2)$$

where the right-hand side contains S, which is the source/sink term that represents all physical processes that generate, dissipate, or redistribute wave energy. The equation of S is as follows:

$$S = S_{in} + S_{ds,w} + S_{ds,b} + S_{ds,br} + S_{nl4} + S_{nl3} \qquad (3)$$

where S_{in} is the term for transferring of wind energy to the waves (Komen et al., 1984), $S_{ds,w}$ is the term for the energy of whitecapping (Komen et al., 1984), $S_{ds,b}$ is the term for the energy of bottom friction (Hasselmann et al., 1973), and $S_{ds,br}$ is the term for the energy of depth-induced breaking.

D. Mathematical Model Group

The MMG (Mathematical Model Group) model, which is widely used to describe a ship's maneuvering motion, was adopted to estimate a ship's location by simulation. The primary features of the MMG model are the division of all hydrodynamic forces and moments working on the vessel's hull, rudder, propeller, and other categories as well as the analysis of their interaction.

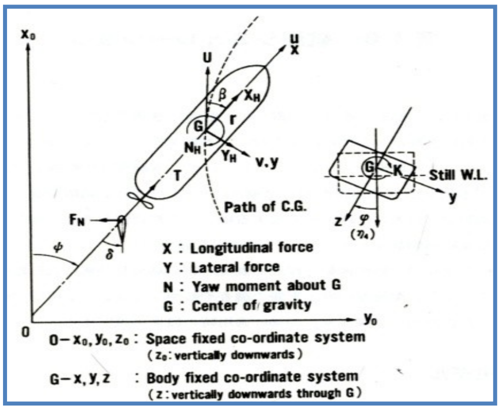

Fig. 1. Coordinate system of MMG

Two coordinate systems are used in ship maneuverability research: space-fixed and body-fixed. In the latter, G-x,y,z, moves together with the ship and is used in the MMG model. In this coordinate system, shown in Fig.1, G is the center of gravity of the ship, the x-axis is the direction the ship is heading, the y-axis is perpendicular to the x-axis on the right-hand side, and the z-axis runs vertically downward through G.

Therefore, the equation of the ship's motion in the body-fixed coordinate system adopted in the MMG is written as:

$$\begin{cases} (m + m_x)u - (m + m_y)vr = X \\ (m + m_y)v + (m + m_x)ur = Y \\ (I_{zz} + J_{zz})r = N \end{cases} \qquad (4)$$

where m is the mass, m_x and m_y are added mass, and u and v are components of velocity in the directions of the x-axis and the y-axis, respectively, and r is the angular acceleration. I_{zz} and J_{zz} are the moment of inertia and the added moment of inertia around G, respectively. X and Y are hydrodynamic forces, and N is the moment around the z-axis.

According to the MMG model, the hydrodynamic forces and the moment in the above equation can be written as:

$$\begin{cases} X = X_H + X_P + X_R + X_T + X_A + X_W + X_E \\ Y = Y_H + Y_P + Y_R + Y_T + Y_A + Y_W + Y_E \\ N = N_H + N_P + N_R + N_T + N_A + N_W + N_E \end{cases} \qquad (5)$$

where the subscripts H, P, R, T, A, W, and E denote the hydrodynamic force or moment induced by the hull, propeller, rudder, thruster, air, wave, and external forces, respectively.

Hydrodynamic forces caused by wind, waves, and currents are defined in (6), (7), and (8), respectively.

$$\begin{cases} X_A = \frac{\rho_A}{2} V_A^2 A_T C_{XA}(\theta_A) \\ Y_A = \frac{\rho_A}{2} V_A^2 A_L C_{YA}(\theta_A) \\ N_A = \frac{\rho_A}{2} V_A^2 L A_L C_{NA}(\theta_A) \end{cases} \qquad (6)$$

where ρ_A is the density of air, θ_A is the relative wind direction, $V_A$is the relative wind velocity, and A_L and A_T are the frontal projected area and lateral projected area, respectively. C_{XA}, C_{YA}, and C_{NA} are the coefficients. In this paper, these coefficients were estimated by the method of Fujiwara et al. as

$$\begin{cases} X_W = \rho g h^2 B^2 / L\overline{C_{XW}}(U, T_V, \aleph - \varphi_0) \\ Y_W = \rho g h^2 B^2 / L\overline{C_{YW}}(\omega_0, \aleph - \varphi_0) \\ N_W = \rho g h^2 B^2 / L\overline{C_{NW}}(\omega_0, \aleph - \varphi_0) \end{cases} \quad (7)$$

Where ρ is the density of seawater, g is the acceleration of gravity, h is the amplitude of significant wave height, B is the ship's breadth, and L is the length of the ship. $\overline{C_{XW}}$, $\overline{C_{YW}}$, and $\overline{C_{NW}}$ are averages of short-term estimated coefficients.

III. SIMULATION AND RESULTS

A. Wind Simulation

The simulation period was from 00:00 UTC, September 2, 2004, to 00:00 UTC, September 8, 2004. Figure 2 shows the weather charts obtained from JMA (Japan Meteorological Agency) when the low pressure was closest to Osaka Bay.

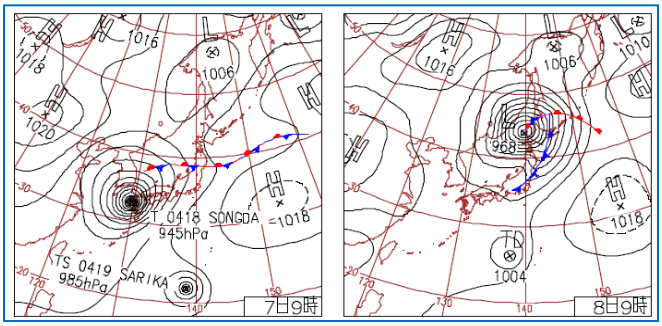

Typhoon: September 7, 8, 00:00 UTC, 2004

Fig. 2. Weather charts of simulated typhoons (JMA)

As shown in Fig.3, two areas for nesting were calculated to simulate winds more accurately. In the calculation, the vertical grid is 28 from top pressure to ground pressure. Compared to the former one (Chen Chen.,et al.2013), we simulate wind by using a higher resolution for both nests, which aimed to obtain a more exact wind velocity, and the detailed information calculated by WRF is shown in Table.1

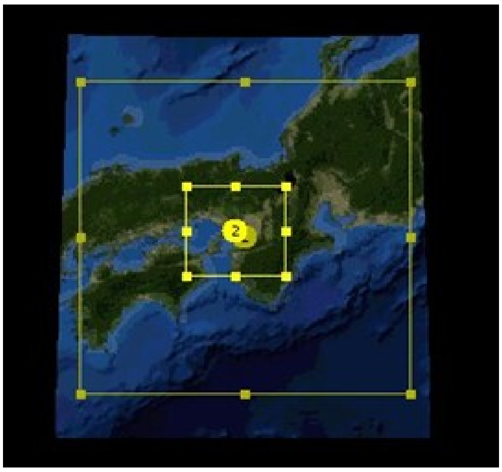

Fig. 3. WRF simulation domains

Table 1. Conditions for calculation by WRF

	Osaka Bay Calculation	
	d01	d02
Dimension	100 x 100 x 28	85 x 88 x 28
Mesh size	4.5km	1.5km
Time step	60 (s)	12 (s)
Start time	2004-09-02-00:00:00 UTC	
End time	2004-09-08-00:00:00 UTC	

As shown in Figure 4 and Figure 5, a strong south wind blew when the low pressure was closest to Osaka Bay. The calculated wind velocity and direction were compared with the observation data from JMA. Both sets of data are mostly consistent closest to Osaka Bay, which was also the time period the ship simulation was conducted. Low resolution of the WRF grid and complicated topography, such as the mountains located around Osaka Bay and the artificial islands along the coastline, may contribute to the difference.

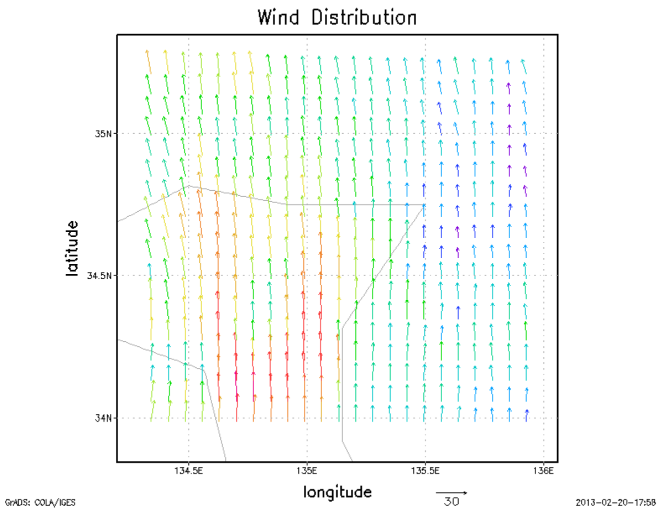

Typhoon Speed and Direction

Fig. 4. Surface wind distributions in Osaka Bay

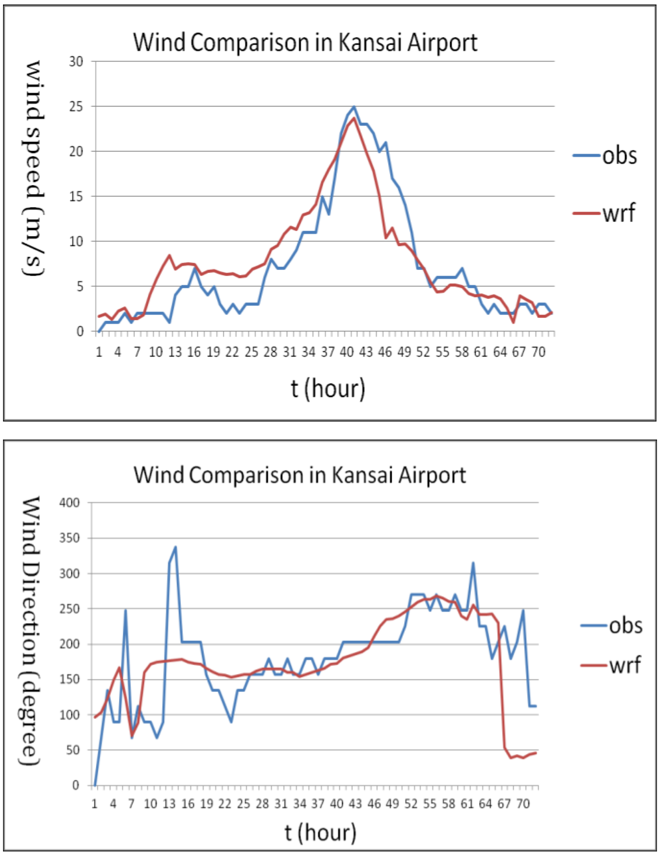

Fig. 5. Comparisons of wind velocity and direction

B. *Current Calculation*

The wind calculated from WRF was applied into the current simulation of POM. The grid resolution in the x and y directions are the regular mesh, while the sigma coordinate system is used in the vertical direction. The grid number is 720 x 600 in the x-y axis. The horizontal grid interval of Δx and Δy is 150m. The calculation time interval is 2 seconds.

The velocity distribution of the surface tidal current in Osaka Bay when the low pressure was closest is shown in Fig.6. The sea level height between observation and POM calculation was compared in Fig.7. The change of surface current distribution, which is the main factor affecting ship navigation, was dramatic.

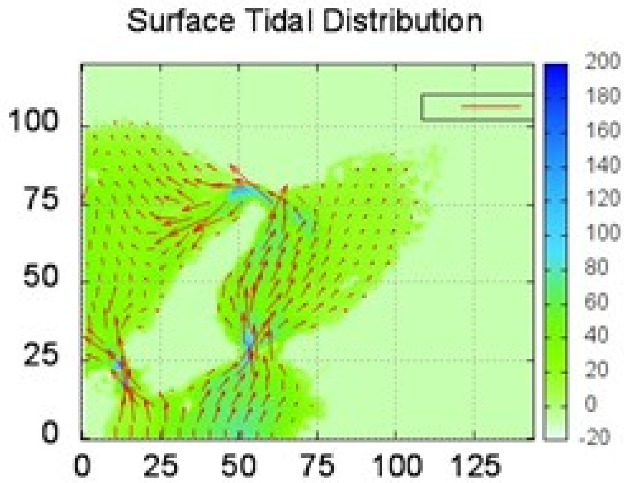

Fig. 6. Surface tidal distributions of tidal current

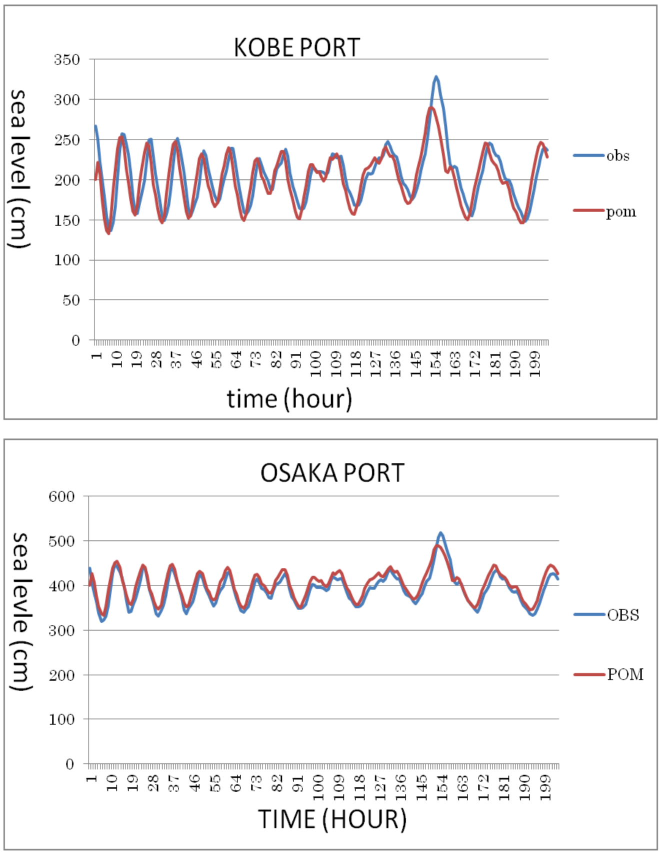

Fig. 7. Comparison of sea level between observation and POM calculation

C. *Wave Calculation*

The numerical simulation of waves was carried out using the SWAN model. The water depth of the regular grid interval of Δx and Δy is 50m. The mesh size is about 0.5 km, and the calculated time step is 5 seconds. The number of frequencies is 30, and the number of meshes in θ is 36.

As shown in Fig.8, the calculated wave height was verified by the observed wave height of NOWPHAS (Nationwide Ocean Wave information network for Ports and HArbourS).

The results of the significant wave height calculation are shown in Fig.9. Comparing the simulation with observation data, we can say that the simulation by SWAN agrees with that of WRF.

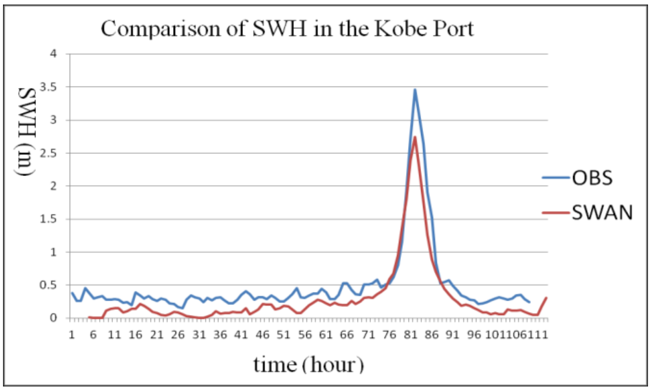

Fig. 8. Comparison of calculated and observed significant wave height

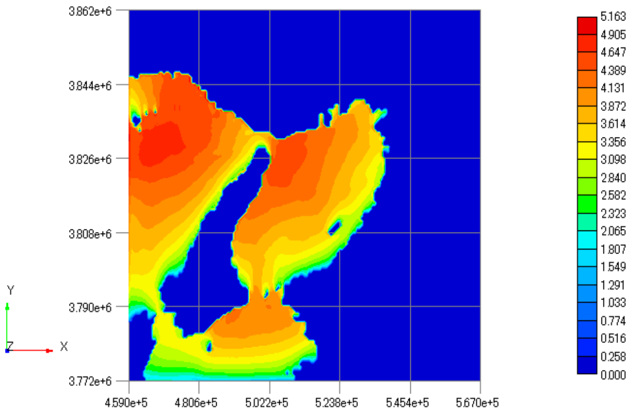

Distribution of Significant wave height (m)

Fig. 9. Simulated ocean waves in Osaka Bay

D. Ship Maneuvering Simulation

Before applying the MMG model, the short-term predictions of the added resistance, wave-induced steady lateral force, and yaw moment in regular waves were obtained using the RIOS (Research Initiative on Oceangoing Ships) system, which was developed at Osaka University.

The MMG simulations were based on the characteristics of a container ship, SR108, with detailed information shown in Table 3. The data of the hull lines and main characteristics of this ship were used for the calculation.

The numerical navigation was carried out with a fixed propeller revolution and a ship speed kept as 20 knots in still water. For all of these simulations, a straight-heading direction was used for about one hour for courses 045 and 225 and for about half an hour for courses 090 and 270 as shown in Figure 10.

The hydrodynamic forces as well as external forces were simplified. Only the advance, drift, and rotation motions in smooth water were considered. In all cases, autopilot was utilized.

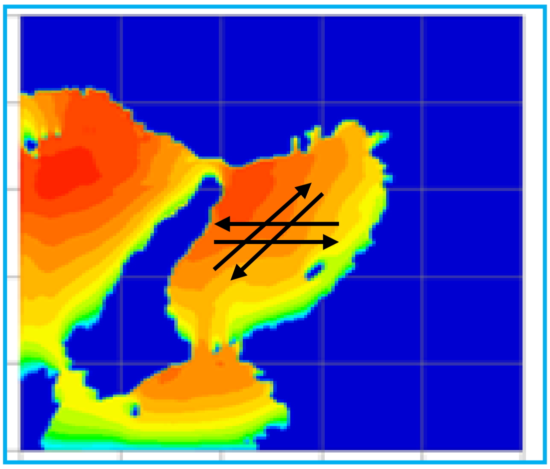

Fig. 10. Virtual course lines for numerical navigation

Table 3. Principal Properties of the SR108

Symbol	Ship
Length (P.P)	175.00m
Length (W.L)	178.21m
Beam (M.L.D)	25.40m
Draught (M.L.D)	9.50m
LCG relative to midships	-2.48m
Block coefficient	0.572
Displaced volume	24,801ton
Wetted surface	5,499m^2
Diameter of propeller	6.507m
Ratio of propeller pitch	0.7348
A_R (m^2)	32.46m^2

In the numerical simulation, the effects of the ship's tracks on the wind waves, tidal currents, wind-wave currents, and set course are shown in Figure 11. The coordinate system in these figures is longitude (E) and latitude (N).

The course line marked with purple star indicates the dead-reckoning track. The line marked with red squares tracks the effects of tidal currents. The line marked with green triangles shows the effect of wind and wave, while the line marked with blue circles shows the influence of a combination of wind, wave, and tidal currents. Obvious influences by these factors can be found by noting the difference of coordinate intervals of longitude (E) and the latitude (N).

For the courses 045 and 225 cases, the enlarged figures of the final navigation period were shown here.

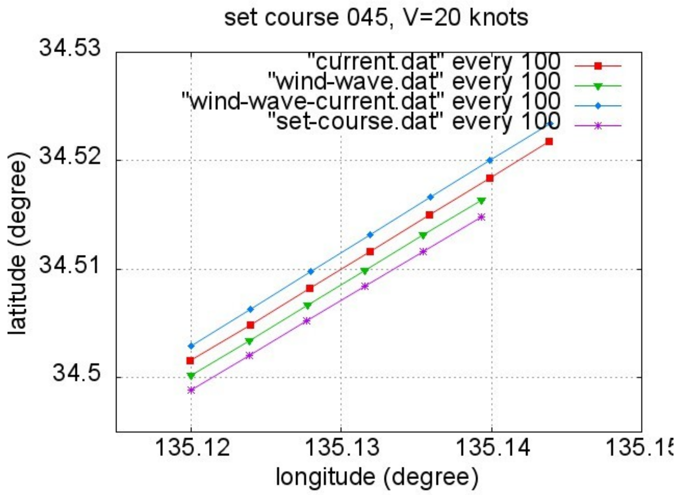

(a) Virtual Course Lines of 045^o

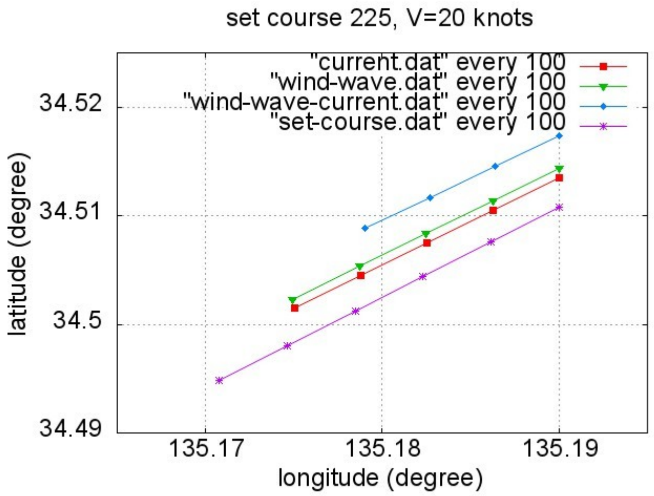

(b) Virtual Course Lines of 225^o

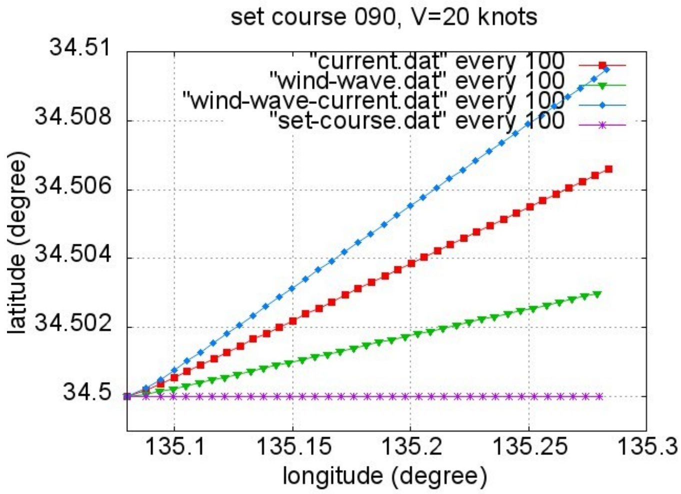

(c) Virtual Course Lines of 090^o

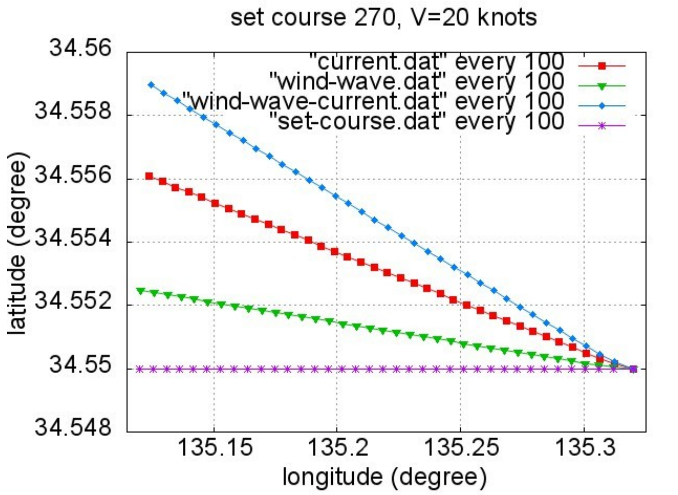

(d) Virtual Course Lines of 270^o

Fig. 11. Numerical ship navigation in Osaka Bay

IV. COMPARISON OF RESULTS AND DISCUSSION

By comparing the actual tracks in four virtual courses, we find that the strong south wind of the typhoon has an effective influence on moving the ship northward. When navigating in and against following currents, as shown in Figures 11 (a) and 11 (b), the ship has a tendency to move a longer- and shorter-than-normal distance, respectively, but moving in a headwind can make the actual distance shorter. Additionally, when ship movement is influenced by lateral waves, as shown in Figures 11 (c) and 11 (d), lateral displacements are relatively large.

Considering the drift tracks above, we can confirm that wind has a major effect on drift distance, while current has a greater influence on drift angle. By comparing the drift angles, we found that the tidal current has a greater effect on a moving ship than the effects of waves and wind.

V. CONCLUSION

With a higher model resolution, these weather and ocean models can work out a better result, which was applied to get the effects on a sailing ship. And the conclusions are as follows:

1) Combining the numerical models WRF, SWAN, and POM, effective and high-resolution data of wind, wave, and current can be generated.

2) Calculated data by higher-resolution calculation can lead to a more exact influence of wind, waves, and currents on an oceangoing vessel.

3) Considering the differences among these factors, the largest effect on the drift angle was found from the tidal current, while the wind has a greater effect on drift distance.

The next step of this research is to conduct a numerical ship simulation combined with the weather and ocean forecast in open sea areas.

ACKNOWLEDGMENT

The authors are grateful for the support of the RIOS model provided by the Division of Global Architecture of Osaka University of Japan, by which the response of ship to wave was performed.

REFERENCES

[1] Blumberg, A. F., and Mellor, G. L., "A description of a three dimensional coastal ocean circulation model. Three-Dimensional Coastal Ocean Models," N. Heaps, Ed., Coastal and Estuarine Series, No. 4, Amer. Geophys. Union, pp. 1-16, 1987.

[2] Mellor, G. L., "User's guide for a three-dimensional, primitive equation, numerical ocean model. Rep.," Program in Atmospheric and Oceanic Science, Princeton University, pp. 41,1998.

[3] Booji, N., et al., "A third-generation wave model for coastal regions, part 1." Model description and validation, J. Geograph. Research, 104, C4, pp.7649-7666,1999..

[4] Whitham, G. B., "Linear and Nonlinear Waves," John Wiley, NewYork, pp. 636, 1974.

[5] Dingemans, M. W., "Water wave propagation over uneven bottoms, part1." Linear wave propagation, Adv. Ser. Ocean Eng., World Sci., River Edge, N. J., Vol. 13, pp. 471,1997.

[6] Komen, G. J., Hasselmann, S., and Hasselmann, K., "On the existence of a fully developed wind-sea spectrum." J. Phys. Oceanography, 14, pp. 1271-1285, 1984.

[7] Hasselmann, K., et al., "Measurements of wind-wave growth and swell decay during the Joint North Sea Wave Project (JONSWAP)." Dtsch. Hydrogr. Z. Suppl., 12(A8), pp. 1-95, 1973.

[8] Fujiwara, T., Ueno, M., and Nimura, T., "Estimation of wind forces and moments acting on ships." Journal of the Society of Naval Architects of Japan (183), pp. 77-90, 1998.

[9] Carvalho, D., Rocha, A., Gomez-Gesteira, M., and Santos, C., "A sensitivity study of the WRF model in wind simulation for an area of high wind energy." Environmental Modeling & Software, 33, pp. 23-34, 2012.

[10] Mase, H., Katsui, S., Yasuda, T., Tomand, T. H., and Ogawa, K., "Verification of GFS-WRF-SWAN wave prediction system by three seasons' comparison." Annual Journal of Civil Engineering in the Ocean, JSCE Vol. 22, p. 109-114, 2006.

[11] The SWAN Team, "SWAN, Scientific and Technical Documentation. SWAN Cycle Ⅲ version 40.72ABC,"

[12] RIOS. Research Initiative on Oceangoing Ships,

[13] Xia, H., Shiotani, S., et al., "A study of weather routing considering real time data of weather and ocean for sailing ship in coastal area –Basic simulation of ship positioning by ship maneuvering and experiment by a real ship." Journal of the Kansai Society of Naval Architects, Japan, No. 234, p. 159-166, 2006.

[14] Xia, H., Shiotani, S., et al., "Estimation of ship's course for sailing on route by navigation simulation in coastal water." The Journal of Japan Institute of Navigation, No. 115, p. 51-57, 2006.

[15] Chen Chen, Shigeaki Shiotani, Kenji Sasa., "Numerical

ship navigation based on weather and ocean simulation." Ocean Engineering, Volume 69, Pages 44–53, 1 September 2013.

[16] Yoshimura, Y., "Mathematical model for the maneuvering ship motion in shallow water." Journal of the Kansai Society of Naval Architects, Japan, No. 200, p. 41-51, 1986.